Published in final edited form as:

Eur J Immunol. 2019 February ; 49(2): 242–254. doi:10.1002/eji.201847717.

Self-glycerophospholipids activate phospholipid-reactive T cells, and interfere with iNKT cell activation by competing with iNKT cell ligands for CD1d loading

Ramesh Chandra Halder[1], **Cynthia Tran**[1], **Priti Prasad**[1,2], **Jing Wang**[3], **Dhiraj Nallapothula**[1], **Tatsuya Ishikawa**[1], **Meiying Wang**[1], **Dirk M. Zajonc**[3,4], and **Ram Raj Singh**[1,2,5,6]

[1]Autoimmunity and Tolerance Laboratory, Division of Rheumatology, Department of Medicine, David Geffen School of Medicine at University of California Los Angeles, Los Angeles, CA 90095, USA

[2]Molecular Toxicology Interdepartmental Program, David Geffen School of Medicine at University of California Los Angeles, Los Angeles, CA 90095, USA

[3]Division of Immune Regulation, La Jolla Institute for Allergy and Immunology, La Jolla, CA 92037, USA

[4]Department of Internal Medicine, Faculty of Medicine and Health Sciences, Ghent University, 9000 Ghent

[5]Jonsson Comprehensive Cancer Center, David Geffen School of Medicine at University of California Los Angeles, Los Angeles, CA 90095, USA

[6]Department of Pathology and Laboratory Medicine, David Geffen School of Medicine at University of California Los Angeles, Los Angeles, CA 90095, USA

Abstract

Glycosphingolipids and glycerophospholipids bind CD1d. Glycosphingolipid-reactive invariant NKT-cells (iNKT) exhibit myriad immune effects, however, little is known about the functions of phospholipid-reactive T-cells (PLT). We report that the normal mouse immune repertoire contains αβ T-cells, which recognize self-glycerophospholipids such as phosphatidic acid (PA) in a CD1d-restricted manner and don't cross-react with iNKT-cell ligands. PA bound to CD1d in the absence of lipid transfer proteins. Upon in vivo priming, PA induced an expansion and activation of T-cells in Ag-specific manner. Crystal structure of the CD1d:PA complex revealed that the ligand is centrally located in the CD1d-binding groove opening for TCR recognition. Moreover, the increased flexibility of the two acyl chains in diacylglycerol ligands and a less stringent binding orientation for glycerophospholipids as compared with the bindings of glycosphingolipids may allow glycerophospholipids to readily occupy CD1d. Indeed, PA competed with α-galactosylceramide to load onto CD1d, leading to reduced expression of CD1d:α-galactosylceramide complexes on the surface of dendritic cells. Consistently, glycerophospholipids reduced iNKT-cell proliferation, expansion, and cytokine production in vitro and in vivo. Such

Corresponding author: Dr. Ram Raj Singh, UCLA Department of Medicine/Rheumatology, 1000 Veteran Avenue, Room 32-59, Los Angeles, CA 90095-1670. Phone number: 310-206-7491; RRSingh@mednet.ucla.edu.

superior ability of self-glycerophospholipids to compete with iNKT-cell ligands to occupy CD1d may help maintain homeostasis between the diverse subsets of lipid-reactive T-cells, with important pathogenetic and therapeutic implications.

Introduction

Lipids are essential components of biological membranes [1]. Glycerol-based phospholipids (PL), called glycerophospholipid (GPL), are the most abundant membrane lipids. They are composed of a glycerol backbone, two fatty acid chains, and a polar headgroup. The glycerol backbone is esterified to phosphoric acid, resulting in the formation of phosphatidic acid (PA), from which all other GPLs are formed by the addition of a polar headgroup like choline, ethanolamine, glycerol, inositol, and serine, producing the main PLs in the cell, namely phosphatidylcholine (PC), phosphatidylethanolamine (PE), phosphatidylglycerol (PG), phosphatidylinositol (PI) and phosphatidylserine (PS), respectively. Glycosphingolipids are another group of membrane lipids that are composed of a ceramide backbone and a sugar moiety. In addition to their many roles in cellular processes such as cell signaling and energy storage [1], these membrane lipids bind Ag presenting molecules CD1d in mice and CD1a-d in humans which present them to T cells that exert profound influence on immunity [2, 3].

Mass spectroscopy studies have identified glycosphingolipids and GPLs as the major groups of self-lipid ligands for CD1d in humans [4]. PC and PE have also been eluted from murine CD1d (mCD1d) [5], and PI has been identified as a cellular ligand of mCD1d [6]. Functional studies have revealed diverse populations of T cells that recognize self-lipids [7–12], including invariant NKT cells (iNKT) reactive to endogenous α-glucosylceramide and to GPLs such as PI, γδ T cells reactive to PE and PC in humans and di-PG (DPG) in mice, and diverse NKT (dNKT) cells reactive to sulfatide. During bacterial infection, modulation of self-lipid metabolism and presentation is sufficient to induce immune response independent of the type of bacteria used [13]. Interestingly, a dNKT cell hybridoma reactive to bacterial GPLs, namely PG and DPG, exhibited cross-reactivity with the homologous mammalian GPLs [14], suggesting a role of self-GPLs in shaping the repertoire of T cells that respond to foreign lipids. Thus, characterization of T cells specific for self-lipids will help elucidate their roles in immunity.

GPLs, including PA, PC, PE, PG, DPG, PI, and PS, have been eluted and identified by mass spectrometry as natural human CD1d ligands [4]. PC and PE have also been eluted from mCD1d [5], and glycosylated PI and unmodified PI have been identified as cellular ligands of mCD1d [6, 15]. Crystallographic studies have shown that complexes of CD1d bound to GPL Ag PC [5], PI dimannoside [16] and DPG [8] can exist, and functional studies have shown that both αβ and γδ T cells can recognize natural and synthetic PLs in a CD1d-restricted manner [8, 14, 17–19]. PL Ag PE and PC from pollens can activate human γδ T cells in a CD1-restricted manner [18–20]; and lyso-PC stimulates cytokine responses by human NKT cell clones and peripheral blood lymphocytes [21]. In mice, PE and PI have been shown to stimulate mCD1d-restricted NKT cell hybridomas [9, 22], and DPG has been shown to stimulate murine γδ T cell and dNKT cell hybridomas [8, 14, 23]. Taken together,

these findings suggest that PLs can serve as natural ligands for CD1d and induce CD1d-restricted T cell responses. However, T cells that recognize abundant self-GPLs appear to be rare in normal immune repertoire, and their biology, distribution, phenotype, and *in vivo* responsiveness are not well understood.

Extensive work using glycosphingolipid α-galactosylceramide (αGalCer)-reactive iNKT cells has demonstrated their roles, both protective and pathogenic, in a wide range of diseases including asthma, atherosclerosis, autoimmune diseases, infection, cancer, and metabolic syndrome [24–27]. The iNKT cell functions have been attributed to their effects in modulating immune response [3, 25]. Upon activation, iNKT cells secrete many cytokines, kill target cells, and modulate B cell functions [3, 28, 29]. However, little is known about the *in vivo* functional roles of T cells reactive to self-GPL Ag.

Here, we identified and characterized self PL-reactive T cells (PLT) using mCD1d tetramers loaded with major self-GPL Ag, and performed cellular analyses, chemical binding, crystal structure, competitive inhibition, and *in vivo* functional studies. We demonstrate that T cells reactive to GPL Ag are a subset of CD1d-restricted T cells that are phenotypically and functionally distinct from iNKT cells, and can exert important immune functions.

Results

T cells that recognize self-GPL Ag exist in the normal immune repertoire

To identify T cells reactive to self-GPLs, we stained spleen and liver mononuclear cells (MNCs) from naïve animals with CD1d tetramers loaded with PBS (control), control glycosphingolipid Ag including αGalCer analog PBS57 and sulfatide, and GPL Ag, namely PA, PC, PE, PI, and PS (Fig. 1A, B, Supplemental Fig. 1). Stained cells were analyzed for tetramer^{+} cells on gated live non-B lymphocytes. In the liver, 0.3% to 1.8% of live lymphocytes stained for GPL/CD1d tetramers and TCRβ, which was comparable to the frequency of sulfatide-reactive dNKT cells, but much less frequent than αGalCer-reactive iNKT cells. In spleen, the frequencies of PLTs, iNKTs and dNKTs were all comparable. 35–70% of PA/CD1d tetramer positive T cells expressed CD4 and NK1.1 (Fig. 1C, D, Supplemental Fig. 1). Thus, PLT cells exist in the normal mouse lymphoid organs.

Binding and presentation of GPL Ag PA to mCD1d

We assessed the binding of PA to mCD1d by native IEF gel electrophoresis (Fig. 2A). Upon incubation of mCD1d with PA, two major bands were apparent. The lower band corresponds to mCD1d containing an uncharged endogenous spacer lipid derived from its expression in insect cells (net charge 0), whereas the upper band corresponds to mCD1d:PA complexes (net charge −1). In addition, purified mCD1d also contains a faint band above the major species of mCD1d. This band is either the result of endogenous ligands with different charge values bound to mCD1d (Fig. 2A, *mCD1d*), or the result of heterogeneity of the mCD1d protein itself, as the band appears to be shifted above the −1 band, when either sulfatide or PA is bound. The binding of PA to mCD1d occurred in the absence of lipid transfer proteins (none were present in the system), although binding was less efficient than that of the positive control (sulfatide). Binding of PA to mCD1d can be enhanced by loading PA in the

absence of detergent (Fig. 2A [*+PA*]), while the addition of 0.05% Tween-20 during incubation showed reduced PA loading (Fig. 2A [*+PA Tween*]), likely a result of PA being sequestered in detergent micelles. Chemical structures of the lipids are shown in Fig. 2B.

To reveal the molecular basis of how PA is bound and presented by mCD1d, we crystallized the mCD1d:PA complex and determined the crystal structure to 2.24 Å resolution (Fig. 2C, D, and Supplemental Table 1). CD1d is formed as a non-covalent heterodimer composed of the CD1d heavy chain and β2-microglobulin. The CD1d heavy chain forms a hydrophobic Ag-binding groove between the α1 and α2-helix that sits above a central β-sheet platform. Ligands are typically bound with their lipid moiety inserted into the binding groove that can further be divided into two binding pockets A′ and F′, each containing a single alkyl chain of a dual-alkyl chain lipid. PA is modeled with the sn-1 oleic acid in the A′ pocket and the sn-2 oleic acid in the F′ pocket (Fig. 2D). However, as both fatty acids chains are identical and considering the slight ambiguity of the electron density, the reverse binding orientation cannot be excluded. Both binding orientations have been observed for other GPLs, such as PI dimannoside and PC (Fig 2E, F). This suggests a less stringent binding orientation for PA to mCD1d, as compared with the binding of ceramide-based ligands, such as αGalCer and sulfatide. The central phosphate group of PA is oriented through H-bond interactions with CD1d residues R79, D153 and T156 but not with D80. Thus, the ligand is centrally located at the CD1d binding groove opening for TCR recognition, similar to the ligands PIM-2 and PC (Fig 2E, F), while the phosphate moiety will serve as the major antigenic moiety for T cell recognition.

PLT cells are distinct from iNKT cells

Next, we asked if PLT cells are distinct from iNKT cells. Consistent with data shown in Fig. 1 and 2, PA/CD1d tetramer^{+} T cells were absent in CD1d$^{-/-}$ mice (Fig. 3A). However, these T cells were present in normal numbers in Jα18$^{-/-}$ mice that lack iNKT cells (Fig. 3B). Furthermore, T cells that recognize CD1d-tetramers loaded with PA did not co-stain with CD1d-tetramers loaded with αGalCer analog PBS57 (Fig. 3C). While αGalCer administration led to reduced iNKT cells at 24h post-injection [30] (Fig. 3D), there was no effect on the frequency of PA-reactive T cells (Fig. 3E). Finally, GPL Ag did not stimulate an iNKT cell hybridoma (Fig. 3F). Thus, PLT cells in the normal mouse lymphoid organs are a distinct subset of CD1d-restricted T cells, which do not cross-react with iNKT cell ligands.

PLT cells respond to in vivo priming with a GPL

To determine if T cells reactive to self-GPLs can be primed *in vivo*, we injected mice with PA. The proportions and numbers of PA/CD1d-tetramer^{+} T cells significantly increased in the liver 24h after an immunization with PA as compared to animals injected with vehicle (Fig. 4A), whereas the frequencies of PBS57/CD1d-tetramer^{+} T cells or of T cells that recognize CD1d tetramers loaded with another GPL antigen, PI, were unaffected by immunization with PA (Fig. 4B). As a corollary to this, immunization with α GalCer did not change the frequency of T cells that recognize PA/CD1d tetramers (Fig. 3E). Incubation of enriched T cells in plates coated with recombinant CD1d followed by PA or PBS also led to significantly higher proportions and total numbers of PA/CD1d-tetramer^{+} T cells in the

presence of PA than of PBS (Supplemental Fig. 2). PA immunization increased the expression of activation marker CD69 on PA-reactive T cells (Fig. 4C) and increased the production of IFNγ by PA-reactive T cells (Fig. 4D, E, Supplemental Fig. 3). However, IFNγ production by iNKT cells was unaffected by PA immunization (Fig. 4F). PA immunization also increased serum levels of IL-4 and IFNγ (Fig. 4G). Thus, PLT cells expand and produce cytokines upon *in vivo* priming with a GPL in an Ag-specific manner.

GPL Ag competes with αGalCer for loading onto mCD1d

A less stringent binding orientation for GPLs, as compared to ceramides, to mCD1d (Fig. 2) suggested that GPLs might efficiently compete with other lipid ligands to load onto mCD1d. To test this, we detected the expression of CD1d:αGalCer complexes on the surface of DCs after incubation of spleen cells with PA, αGalCer, or both. Co-incubation with PA and αGalCer reduced the expression of CD1d:αGalCer complexes, but not of CD1d, compared to when cells were incubated with αGalCer alone (Fig. 5A). A similar reduction in CD1d:αGalCer complex expression was seen *ex vivo* when animals were injected 24h ago with αGalCer+PA compared to mice injected with αGalCer alone (Fig. 5B). These data suggest that PA competes with αGalCer for loading onto CD1d.

To further test if GPL Ag compete with αGalCer for presentation by CD1d, we performed a competitive inhibition assay where we coated plates with soluble mCD1d prior to incubation with αGalCer and/or PA and culture with iNKT hybridoma cells. As shown in Fig. 5C, co-incubation with PA markedly reduced the activation of iNKT cells in a dose-dependent manner.

GPLs reduce iNKT cell proliferation

Since PA efficiently competes with αGalCer to load onto mCD1d (Fig. 5), it may reduce αGalCer-induced iNKT cell responses. To test this, we labeled spleen cells from naïve animals with CFSE, and cultured them with αGalCer in the presence or absence of PA. The proliferation of iNKT cells was dramatically reduced in the presence of PA *in vitro* (Fig. 6A). Spleen cells from PA-injected mice also had a markedly reduced proliferation when cultured with αGalCer *ex vivo* (Fig. 6B). Furthermore, αGalCer-induced iNKT cell expansion was curtailed in animals co-injected with PA + αGalCer (Fig. 6C). αGalCer-induced in vitro proliferation of iNKT cells was also inhibited by the addition of other GPL Ag, including PC, PE, PI, and PS, to the splenocytes (Supplemental Fig. 4A). Finally, the reduced iNKT cell responses induced by *in vivo* exposure to GPL Ag could be reversed by IL-2 (Fig. 6D). Thus, GPL-induced reduced iNKT cell proliferation is not due to GPL's non-specific toxicity on iNKT cells.

GPLs reduce cytokine production by iNKT cells

Next, we determined if GPL Ag would reduce cytokine production by iNKT cells. Indeed, IFNγ and IL-4 producing iNKT cells were reduced in mice co-injected with αGalCer+PA compared to mice injected with αGalCer alone (Fig. 7A-C). Other GPL Ag tested, including PC, PE, PI, and PS, also reduced αGalCer-induced IFNγ and IL-4 release by spleen cells in vitro (Supplemental Fig. 4B). However, addition of PA alone or PA+αGalCer to spleen cell cultures did not affect cell viability (Supplemental Fig. 4C). The inhibitory capacity of GPLs

must be robust *in vivo*, as serum levels of IFNγ and IL-4 were also lower in mice injected with αGalCer+PA than with αGalCer alone (Fig. 7D). Thus, GPL Ag significantly reduce cytokine responses by iNKT cells.

Discussion

We report that CD1d-restricted T cells reactive to self-GPLs exist in the normal immune repertoire and are phenotypically and functionally distinct from iNKT cells. *In vivo* priming with a GPL Ag led to expansion of GPL Ag-reactive T cells that produced IFN-γ. Chemical binding, structural, and loading studies showed that a GPL binds to mCD1d in the absence of lipid transfer proteins, occupies mCD1d-binding groove opening in the central location, and competes with an iNKT cell ligand to load onto mCD1d. Consequently, treatment with GPLs resulted in reduced iNKT cell proliferation and cytokine production. Such ability of self-GPLs to compete with iNKT cell ligands to occupy CD1d may help maintain homeostasis between the diverse subsets of CD1d-restricted T cells.

Many self-lipids that bind CD1d have been reported to stimulate iNKT cells [22, 31, 32]. For example, ether-bonded lyso-PA and plasmalogen lyso-PE isolated from thymus stimulated iNKT cells [32]. Lyso-PC also stimulated human iNKT cell clones and lines [21], but did not activate mouse iNKT cell hybridomas [33]. However, accumulating evidence suggests that although murine iNKT cells can sometimes recognize self-lipids such as PI, PE, and PG [9, 22, 32], the reactivity to the GPL Ag is generally weak and limited to a few iNKT cell clones. While differences in the requirements for loading self-Ag onto human vs. murine CD1d [34] may explain some differences between mouse and human iNKT cell activation by self-ligands, self-GPLs may serve as ligands for other subsets of CD1d-restricted T cells. For example, lyso-PC can activate dNKT cells that express diverse TCR αβ repertoire in humans [17], and γδ T cells can recognize DPG in mice [8]. Thus, self-lipids including GPLs can act as endogenous ligands for different subsets of CD1d-restricted T cells, including iNKT, dNKT, and γδ-T cells. We demonstrate that mouse lymphoid organs contain a population of T cells that recognize CD1d tetramers loaded with self-GPLs including PA, PC, PE, PI, and PS. Such PLT cells neither overlap with iNKT cells in tetramer binding nor recognize iNKT cell ligand αGalCer. Thus, T cells that recognize self-GPL Ag bound to CD1d molecules form part of self T cell repertoire in normal mice.

We demonstrate that the *in vivo* priming with PA enhanced the frequency of PA/CD1d tetramer$^+$ T cells, activated them, and increased cytokine production, but did not activate iNKT and conventional T cells or T cells reactive to other GPLs. γδ T cells that respond to bacterial or mammalian DPG also secrete IFN-γ [8]. Thus, the normal immune repertoire contains T cells that respond to self-GPLs in an Ag-specific manner.

Chemical and structural analyses revealed that the binding of a GPL, PA, to mCD1d occurred in the absence of lipid transfer proteins, and GPL Ag have been shown to readily occupy the CD1d binding groove presumably to stabilize the CD1d during protein folding in the endoplasmic reticulum [34]. As such, GPLs are continuously found associated with CD1d, which may keep PLT cells tolerized, thus explaining a modest T cell activation response to self-GPLs. A comparison of mCD1d binding of PA to that of other mCD1d

ligands reveals that the lipid backbone of the various lipids binds slightly differently inside mCD1d and therefore leads to a slightly different presentation of the polar moieties for recognition by specific T cells. The binding of the diacylglycerolipid backbones appears less conserved than the binding of the glycosphingolipid backbones [35]. Although, the mCD1d binding of PA and other GPLs, namely PC, PI, a mannosylated PI, and DPG, appears quite similar [5, 8, 35, 36], the position of the proximal phosphate is slightly different in different mCD1d-GPL crystal structures, which affects the presentation of the headgroup. Different from most of previously described self-lipids, PA is a unique lipid in that it has a small highly-charged headgroup that forms fewer hydrogen bonds with CD1d.

Since both fatty acids chains of PA are identical and considering the slight ambiguity of the electron density, PA and other diacylglycerol ligands can adopt different binding orientations in the groove, with the sn-1or sn-2 linked acyl chains being bound in either pocket. The binding mode is likely dictated by the preference of each pocket for a particular combination of chain length and/or unsaturation degree [37]. The increased flexibility of the two acyl chains in diacylglycerol ligands and generally a less stringent binding orientation for glycerolipids as compared with the bindings of glycosphingolipids may allow GPL ligands to readily occupy CD1d. Indeed, PA competed efficiently with αGalCer for loading onto mCD1d, leading to reduced expression of CD1d:αGalCer complexes on the surface of DCs and reduced iNKT cell activation in a dose-dependent manner. PA may also form more stable complexes with CD1d, which may have a higher half-life *in vivo* than CD1d:αGalCer complexes. However, at this time, we are not able to confidently measure CD1d-PA affinity and binding kinetics, as it also depends on solubility of lipids. Another possibility is that GPLs may replace other lipids bound to CD1d, similar to a detergent molecule. Short-chain PLs are in fact endowed with detergent-like properties [38], although it is not known whether PA or other GPL Ag can act as detergents. Nevertheless, a superior ability of self-GPLs to compete with glycosphingolipid ligands may help maintain homeostasis between the diverse subsets of lipid-reactive T cells.

Although PLT cells exhibited a modest cytokine response, *in vitro* or *in vivo* exposure to GPLs reduced iNKT cell proliferation and cytokine production. Such iNKT cell hyporesponsiveness was reversed in the presence of IL-2, thus GPLs didn’t cause a complete, non-specific inhibition of iNKT cells. Hyporesponsiveness of iNKT cells also occurs in humans and animals with dyslipidemia [39], cancers [27], and autoimmune diseases [26], which is purported to occur due to chronic iNKT cell activation by self-lipids. The latter is extrapolated from the finding that the repeated stimulation by αGalCer induces iNKT cell unresponsiveness [40]. However, *in vivo* or *in vitro* exposure to GPLs did not activate iNKT cells, and a single exposure to GPLs was sufficient to elicit iNKT cell unresponsiveness. Thus, GPL-induced iNKT cell unresponsiveness is not owing to repeated iNKT cell stimulation.

iNKT cell insufficiency develops spontaneously in cancers [27, 41], dyslipidemia [39], lupus [26], and multiple sclerosis [42]. Elucidating mechanisms of reduced iNKT cell responses using the GPL model may have implications for understanding iNKT cell defects and their role in these diseases. It is also possible to speculate that iNKT cell insufficiency in these disorders might occur due to alterations in self-GPLs. The GPL-mediated inhibition of

iNKTs can also have therapeutic implications in diseases where iNKT cells can promote diseases such as atherosclerosis and alcoholic hepatitis [24, 25] or conditions where iNKTs can be protective such as cancers, obesity, and autoimmune diseases [24, 26, 27, 39]. Similar mechanisms might operate in other conditions with altered lipid metabolism [43]. For example, a nonantigenic glycosphingolipid globotriaosylceramide (Gb3), which accumulates in patients with Fabry disease, inhibits iNKT cell activation by competing with exogenous and endogenous Ag for CD1d binding [44]. Furthermore, treatment that reduces Gb3 storage prevents iNKT cell decrease in Fabry disease mice [45]. Variations in plasma GPLs have been found in conditions such as liver cirrhosis [46] and Alzheimer's disease [47, 48], and synovial fluid GPL levels are increased in patients with osteoarthritis [49]. Although the mechanisms by which altered lipid metabolism might affect the development of these diseases remain unclear, this and other studies on GPL-reactive T cells lay the foundation for assessing a role of T cells reactive to self and altered GPLs in the pathogenesis of these diseases.

GPLs, such as PA, are membrane lipids produced by activated macrophages [50], immature DCs [51] and other cell types, and regulate many cellular processes. We identify a new role for self-GPLs and elucidate a mechanism whereby they may regulate immunity. Specifically, GPLs activate a subset of CD1d-restricted PLT cells, but interfere with iNKT cell activation via the ability to compete with iNKT cell ligand to occupy CD1d. Thus, normal lipid metabolism may help maintain the balance between different subsets of lipid-reactive T cells. Such homeostatic balance may be lost in conditions with altered lipid metabolism. Understanding these mechanisms will have therapeutic implications for a wide range of diseases.

Materials and Methods

Animals

Breeding pairs of C57BL/6 (B6), B6 CD1d$^{-/-}$ mice [52], and BALB/c Jα18$^{-/-}$ mice that are deficient for iNKT cells [53] were obtained from the Jackson Laboratory or kindly provided by other investigators, and bred locally. Results from 8–18-week-old locally bred female mice are shown. All mice were maintained in specific pathogen-free conditions. All experiments were approved by the Institutional Animal Care and Use Committee.

Preparation of lipids

Lipid Ag were purchased from Avanti Polar Lipids Inc. (Alabama, USA). αGalCer was dissolved in vehicle (5.6% sucrose, 0.75% L-histidine and 0.5% Tween-20) and incubated at 60°C for 10 min. GPLs in chloroform or vehicle in equivalent volume of chloroform were dried down in a round-bottom glass tube under nitrogen gas and the resultant lipid film dissolved in vehicle and incubated at 60°C for 10 min, which rendered a clear lipid solution. The lipids were further resuspended in complete RPMI 1640 medium (10% FBS, 2 mM L-glutamine, 100 U/ml penicillin streptomycin, 10 mM HEPES, and 5×10^{-5}–5×10^{-6} M 2-ME) for *in vitro* studies or in PBS for animal injections, and vortexed vigorously.

mCD1d tetramers

PE-conjugated unloaded and PBS57-loaded mCD1d tetramers were obtained from the NIH Tetramer Core Facility (Emory, GA). To prepare GPL and sulfatide loaded tetramers, unloaded mCD1d tetramer was mixed with lipid Ag at a molar ratio of 1:3 (protein:lipid) and incubated overnight at room temperature. GPL and sulfatide loaded CD1d tetramers were freshly prepared each time before the experiment.

In vitro loading of lipid Ag

Aliquots of 10 μl purified mCD1d at a concentration of 20 μM were loaded overnight at room temperature in the presence of 6-times molar excess of each lipid. Sulfatide was dissolved in DMSO (5 mg/ml), and PA was dissolved in $CHCL_3$ (10 mg/ml). Loading was performed in the presence of 100 mM Tris-HCl (pH 7). After lipid loading, samples were centrifuged (14,000×*g*, 10 min), and 4 μl supernatant was used for isoelectric focusing (IEF) analysis. CD1d–lipid complexes were separated using precast gels (PhastGel 5–8 IEF) and the PhastSystem (GE Healthcare Biosciences, Piscataway, NJ). Staining of mCD1d was performed with Coomassie blue, and successful lipid loading was identified by a gel shift of the mCD1d band in relation to the control lanes.

Protein expression, purification, and crystallization

Recombinant mCD1d was produced in SF9 insect cells and purified as reported [37]. For structural studies, 2 mg of mCD1d were incubated overnight at room temperature with 0.175 mg of PA (5 mg/ml in $CHCL_3$) in 2 ml of 50 mM Hepes pH 7.5, 150 mM NaCl, resulting in a final $CHCL_3$ concentration of 1.75%, which was tolerated by the protein. After lipid loading, the protein/lipid solution was clarified by centrifugation (17,000xg for 10 min) and the mCD1d:PA complex was purified by size exclusion chromatography using Superdex S200 HR 16/60 in 50mM Hepes, pH 7.5, 150 mM NaCl. Fractions containing mCD1d-PA were pooled and concentrated to 8 mg/ml in 10 mM Hepes pH 7.5, 30 mM NaCl and subjected to crystallization by conventional sitting drop vapor diffusion using commercial crystallization screens (Wizard 1 and 3 from Emerald Biosciences and PEG/Ion 1 and 2) at both 22.3°C and 4°C. Best crystals were manually grown over several days at 4°C by mixing 0.5 μl protein with 0.5μl precipitant (20% polyethylene glycol 4000, 200 mM ammonium acetate).

Structure determination and presentation

Crystals were flash-cooled at 100K in mother liquor containing 20% glycerol. Diffraction data were collected at the Stanford Synchrotron Radiation Lightsource (SSRL) beamline 11–1. Data processing and structure determination by molecular replacement using the mCD1d coordinates from PDB ID 2Q7Y were carried out as reported for other CD1d-glycosphingolipid complexes [54]. Model building and refinement was performed analogous to other CD1d-glycosphingolipid structures [54]. Data collection and refinement statistics are presented in Supplemental Table 1. Structural illustrations were generated using the software PyMol (Schroedinger). Structure factors and coordinates are available from the PDB (http://www.rcsb.org) under accession code 4MX7.

Cell isolation

Hepatic leukocytes were isolated using the Percoll gradient, as previously described [10]. Briefly, following anesthesia with isofluorane (Baxter, Deerfield, IL), mice were perfused with chilled PBS. Liver was removed, cut into small pieces which were passed through a 70 μm nylon cell strainer (BD, Falcon™, Bedford, MA), and suspended in DMEM with 2% heat-inactivated FBS. Cells were washed with medium (850xg for 10 min). Liver MNCs were isolated on a percoll (35% percoll containing 100 U/ml heparin) gradient (850xg for 15 min) and washed twice followed by removal of erythrocytes using RBC lysing buffer (Sigma-Aldrich, St. Louis, MO) and resuspension of cell pellets in medium. BM cells from femur and tibia were obtained by cutting the ends of the bones and forcing medium through the bone shaft, followed by erythrocyte lysis. Spleen cells were obtained by passing through a 70 μm cell strainer, followed by RBC lysis (spleen cells), washing twice and resuspending cells in medium.

Flow cytometry

Cells were suspended in FACS buffer (1–2 × 10^6/ml) containing PBS in 0.02% NaN_3 (wt/vol) and 2% FBS (vol/vol). Cells were first incubated with anti-Fcγ receptor Ab (2.4G2) (BD Biosciences, San Diego, CA) and then labeled with the indicated Ab (Supplemental Information, List of antibodies used). For intracellular cytokine staining, cells were cultured for 5–6h with 500 ng/ml ionomycin and 10 ng/ml PMA in presence of Golgi-plug (1 μl/ml). Cells were harvested, washed and intracellular staining was performed according to the manufacturer's protocol (BD Biosciences). Data were analyzed using FlowJo software (Ashland, OR) with lymphocyte gate, based on forward and side scatter.

Activation of iNKT cell hybridoma

Soluble mCD1d (1 μg/well) was coated onto flat-bottom 96-well plates for 18h at 4°C in PBS (pH 7.4). Plates were washed thrice with PBS, and incubated at 37°C with PBS alone, αGalCer or GPL Ag. For competition assays, PA was added at the indicated concentrations (5–40 μg/ml) to some wells immediately before adding αGalCer. After 4h of incubation with lipids, plates were washed thrice with PBS, followed by addition of 1.5 × 10^5 Hy-1.2 (iNKT cell hybridoma) cells per well in triplicates. Supernatants were collected after 17h and assayed for IL-2 by ELISA.

In vivo lipid treatment

B6 mice were injected i.p. with αGalCer (2–4 μg) or PA (20 μg), and bled and/or euthanized for serum collection and organ harvesting at the indicated timepoints.

CFSE dilution assay to assess proliferation

Splenocytes were labeled with 5 μM CFSE (Molecular Probes, Eugene Oregon) for 10 min at 37^0C in PBS containing 0.1% BSA, and washed twice with complete RPMI medium. Labeled splenocytes (3 × 10^5 cells/well) were then cultured without or with αGalCer (0.1–100 ng/ml) and/or varying concentrations of GPL Ag for 96h in complete RPMI. At the end of the culture, cells were harvested, stained with anti-TCRβ-Cychrome and PBS57/CD1d-

PE and analyzed by flow cytometry. After excluding dead cells using forward and side scatter, CFSE dilution was analyzed on PBS57/CD1d tetramer$^+$ T cells.

Measurement of proliferation response by Ki-67

$4–5\times10^5$ splenocytes were cultured for 96h in the presence of graded concentration of αGalCer (0.1–100 ng/ml) without or with 20 μg of PA. In some experiments, splenocytes were cultured in the presence of graded concentration of different GPLs (2.5–40 μg), with or without 20 ng αGalCer. Cells were harvested, washed and intracellular staining for Ki-67 was performed according to the manufacturer's protocol (BD Biosciences). Ki-67 is expressed by proliferating cells in late G_1, S, G_2 and M phases, but not in resting cells in G_0. After excluding dead cells using forward and side scatter, Ki-67 expression was analyzed on gated PBS57/CD1d tetramer$^+$ cells.

ELISA

Serum was collected and stored at –20°C until use. IFN-γ, IL-4, and IL-17 levels were measured at different time points using sandwich ELISA.

Statistics

Data were analyzed using two-tailed Student's *t* test using Prism software (version 5; GraphPad Software). A *P* value less than 0.05 was considered significant.

Supplementary Material

Refer to Web version on PubMed Central for supplementary material.

Acknowledgements

We thank L. Van Kaer/V. Parekh (Nashville, TN) and M. Taniguchi (Yokohama, Japan) for providing CD1d$^{-/-}$ and Jα18$^{-/-}$ mice, respectively. We thank Stanford Synchrotron Radiation Lightsource (SSRL) beamline 11.1 staff for their kind support. Portions of this research were carried out at the SSRL, a Directorate of SLAC National Accelerator Laboratory and an Office of Science User Facility operated for the U.S. Department of Energy Office of Science by Stanford University.

The study is supported in part by NIH R21 HD082812, R01 AI080778, R01 AR56465, R03 HD067413, R01 AI074952, and Oppenheimer Seed Grant from David Geffen School of Medicine. C.T. and P.P. were supported by Rheumatology Research Foundation Graduate Student Preceptorship awards. P.P. was supported by NIH T32 ES015457. C.T. is supported by NIH F31 AR063603. The SSRL Structural Molecular Biology Program is supported by the DOE Office of Biological and Environmental Research, and by the National Institutes of Health, National Institute of General Medical Sciences (including P41GM103393) and the National Center for Research Resources (P41RR001209).

Abbreviations used in this article

αGalCer	α-galactosylceramide
B6	C57BL/6
DC	dendritic cell
dNKT	diverse NKT

DPG	di-phosphatidylglycerol
GPL	glycerophospholipid
iNKT	invariant NKT
MNC	mononuclear cell
PA	phosphatidic acid
PC	phosphatidylcholine
PE	phosphatidylethanolamine
PG	phosphatidylglycerol
PI	phosphatidylinositol
PL	phospholipid
PLT	phospholipid-reactive T cells
PS	phosphatidylserine

REFERENCES

1. van Meer G, Voelker DR and Feigenson GW, Membrane lipids: where they are and how they behave. Nat Rev Mol Cell Biol 2008 9: 112–124. [PubMed: 18216768]
2. De Libero G and Mori L, Structure and biology of self lipid antigens. Curr Top Microbiol Immunol 2007 314: 51–72.
3. Brennan PJ, Brigl M and Brenner MB, Invariant natural killer T cells: an innate activation scheme linked to diverse effector functions. Nat Rev Immunol 2013 13: 101–117. [PubMed: 23334244]
4. Cox D, Fox L, Tian R, Bardet W, Skaley M, Mojsilovic D, Gumperz J and Hildebrand W, Determination of cellular lipids bound to human CD1d molecules. PLoS One 2009 4: e5325. [PubMed: 19415116]
5. Giabbai B, Sidobre S, Crispin MD, Sanchez-Ruiz Y, Bachi A, Kronenberg M, Wilson IA and Degano M, Crystal structure of mouse CD1d bound to the self ligand phosphatidylcholine: a molecular basis for NKT cell activation. J Immunol 2005 175: 977–984. [PubMed: 16002697]
6. Joyce S, Woods AS, Yewdell JW, Bennink JR, De Silva AD, Boesteanu A, Balk SP, Cotter RJ and Brutkiewicz RR, Natural ligand of mouse CD1d1: cellular glycosylphosphatidylinositol. Science 1998 279: 1541–1544. [PubMed: 9488653]
7. Rossjohn J, Pellicci DG, Patel O, Gapin L and Godfrey DI, Recognition of CD1d-restricted antigens by natural killer T cells. Nat Rev Immunol 2012 12: 845–857. [PubMed: 23154222]
8. Dieude M, Striegl H, Tyznik AJ, Wang J, Behar SM, Piccirillo CA, Levine JS, Zajonc DM and Rauch J, Cardiolipin binds to CD1d and stimulates CD1d-restricted gammadelta T cells in the normal murine repertoire. J Immunol 2011 186: 4771–4781. [PubMed: 21389252]
9. Gumperz JE, Roy C, Makowska A, Lum D, Sugita M, Podrebarac T, Koezuka Y, Porcelli SA, Cardell S, Brenner MB and Behar SM, Murine CD1d-restricted T cell recognition of cellular lipids. Immunity 2000 12: 211–221. [PubMed: 10714687]
10. Halder RC, Aguilera C, Maricic I and Kumar V, Type II NKT cell-mediated anergy induction in type I NKT cells prevents inflammatory liver disease. J Clin Invest 2007 117: 2302–2312. [PubMed: 17641782]
11. Brennan PJ, Tatituri RV, Heiss C, Watts GF, Hsu FF, Veerapen N, Cox LR, Azadi P, Besra GS and Brenner MB, Activation of iNKT cells by a distinct constituent of the endogenous

glucosylceramide fraction. Proc Natl Acad Sci U S A 2014 111: 13433–13438. [PubMed: 25197085]

12. Kain L, Webb B, Anderson BL, Deng S, Holt M, Costanzo A, Zhao M, Self K, Teyton A, Everett C, Kronenberg M, Zajonc DM, Bendelac A, Savage PB and Teyton L, The identification of the endogenous ligands of natural killer T cells reveals the presence of mammalian alpha-linked glycosylceramides. Immunity 2014 41: 543–554. [PubMed: 25367571]
13. De Libero G, Moran AP, Gober HJ, Rossy E, Shamshiev A, Chelnokova O, Mazorra Z, Vendetti S, Sacchi A, Prendergast MM, Sansano S, Tonevitsky A, Landmann R and Mori L, Bacterial infections promote T cell recognition of self-glycolipids. Immunity 2005 22: 763–772. [PubMed: 15963790]
14. Tatituri RV, Watts GF, Bhowruth V, Barton N, Rothchild A, Hsu FF, Almeida CF, Cox LR, Eggeling L, Cardell S, Rossjohn J, Godfrey DI, Behar SM, Besra GS, Brenner MB and Brigl M, Recognition of microbial and mammalian phospholipid antigens by NKT cells with diverse TCRs. Proc Natl Acad Sci U S A 2013 110: 1827–1832. [PubMed: 23307809]
15. De Silva AD, Park JJ, Matsuki N, Stanic AK, Brutkiewicz RR, Medof ME and Joyce S, Lipid protein interactions: the assembly of CD1d1 with cellular phospholipids occurs in the endoplasmic reticulum. J Immunol 2002 168: 723–733. [PubMed: 11777966]
16. Zajonc DM, Ainge GD, Painter GF, Severn WB and Wilson IA, Structural characterization of mycobacterial phosphatidylinositol mannoside binding to mouse CD1d. J Immunol 2006 177: 4577–4583. [PubMed: 16982895]
17. Chang DH, Deng H, Matthews P, Krasovsky J, Ragupathi G, Spisek R, Mazumder A, Vesole DH, Jagannath S and Dhodapkar MV, Inflammation-associated lysophospholipids as ligands for CD1d-restricted T cells in human cancer. Blood 2008 112: 1308–1316. [PubMed: 18535199]
18. Russano AM, Agea E, Corazzi L, Postle AD, De Libero G, Porcelli S, de Benedictis FM and Spinozzi F, Recognition of pollen-derived phosphatidyl-ethanolamine by human CD1d-restricted gamma delta T cells. J Allergy Clin Immunol 2006 117: 1178–1184. [PubMed: 16675349]
19. Russano AM, Bassotti G, Agea E, Bistoni O, Mazzocchi A, Morelli A, Porcelli SA and Spinozzi F, CD1-restricted recognition of exogenous and self-lipid antigens by duodenal gammadelta+ T lymphocytes. J Immunol 2007 178: 3620–3626. [PubMed: 17339459]
20. Agea E, Russano A, Bistoni O, Mannucci R, Nicoletti I, Corazzi L, Postle AD, De Libero G, Porcelli SA and Spinozzi F, Human CD1-restricted T cell recognition of lipids from pollens. J Exp Med 2005 202: 295–308. [PubMed: 16009719]
21. Fox LM, Cox DG, Lockridge JL, Wang X, Chen X, Scharf L, Trott DL, Ndonye RM, Veerapen N, Besra GS, Howell AR, Cook ME, Adams EJ, Hildebrand WH and Gumperz JE, Recognition of lyso-phospholipids by human natural killer T lymphocytes. PLoS Biol 2009 7: e1000228. [PubMed: 19859526]
22. Rauch J, Gumperz J, Robinson C, Skold M, Roy C, Young DC, Lafleur M, Moody DB, Brenner MB, Costello CE and Behar SM, Structural features of the acyl chain determine self-phospholipid antigen recognition by a CD1d-restricted invariant NKT (iNKT) cell. J Biol Chem 2003 278: 47508–47515. [PubMed: 12963715]
23. Born WK, Vollmer M, Reardon C, Matsuura E, Voelker DR, Giclas PC and O'Brien RL, Hybridomas expressing gammadelta T-cell receptors respond to cardiolipin and beta2-glycoprotein 1 (apolipoprotein H). Scand J Immunol 2003 58: 374–381. [PubMed: 12950685]
24. Berzins SP, Smyth MJ and Baxter AG, Presumed guilty: natural killer T cell defects and human disease. Nat Rev Immunol 2011 11: 131–142. [PubMed: 21267014]
25. Tupin E, Nicoletti A, Elhage R, Rudling M, Ljunggren HG, Hansson GK and Berne GP, CD1d-dependent activation of NKT cells aggravates atherosclerosis. J Exp Med 2004 199: 417–422. [PubMed: 14744994]
26. Yang JQ, Saxena V, Xu H, Van Kaer L, Wang CR and Singh RR, Repeated α-galactosylceramide administration results in expansion of NK T cells and alleviates inflammatory dermatitis in MRL-lpr/lpr mice. J Immunol 2003 171: 4439–4446. [PubMed: 14530371]
27. Yanagisawa K, Seino K, Ishikawa Y, Nozue M, Todoroki T and Fukao K, Impaired proliferative response of V alpha 24 NKT cells from cancer patients against alpha-galactosylceramide. J Immunol 2002 168: 6494–6499. [PubMed: 12055270]

28. Yang JQ, Wen X, Kim PJ and Singh RR, Invariant NKT cells inhibit autoreactive B cells in a contact- and CD1d-dependent manner. J Immunol 2011 186: 1512–1520. [PubMed: 21209282]
29. Wen X, Yang JQ, Kim PJ and Singh RR, Homeostatic regulation of marginal zone B cells by invariant natural killer T cells. PLoS One 2011 6: e26536. [PubMed: 22046304]
30. Crowe NY, Uldrich AP, Kyparissoudis K, Hammond KJ, Hayakawa Y, Sidobre S, Keating R, Kronenberg M, Smyth MJ and Godfrey DI, Glycolipid antigen drives rapid expansion and sustained cytokine production by NK T cells. J Immunol 2003 171: 4020–4027. [PubMed: 14530322]
31. Mallevaey T and Selvanantham T, Strategy of lipid recognition by invariant natural killer T cells: 'one for all and all for one'. Immunology 2012 136: 273–282. [PubMed: 22671023]
32. Facciotti F, Ramanjaneyulu GS, Lepore M, Sansano S, Cavallari M, Kistowska M, Forss-Petter S, Ni G, Colone A, Singhal A, Berger J, Xia C, Mori L and De Libero G, Peroxisome-derived lipids are self antigens that stimulate invariant natural killer T cells in the thymus. Nat Immunol 2012 13: 474–480. [PubMed: 22426352]
33. Pei B, Speak AO, Shepherd D, Butters T, Cerundolo V, Platt FM and Kronenberg M, Diverse endogenous antigens for mouse NKT cells: self-antigens that are not glycosphingolipids. J Immunol 2011 186: 1348–1360. [PubMed: 21191069]
34. Salio M, Silk JD and Cerundolo V, Recent advances in processing and presentation of CD1 bound lipid antigens. Curr Opin Immunol 2010 22: 81–88.
35. Zajonc DM and Kronenberg M, CD1 mediated T cell recognition of glycolipids. Curr Opin Struct Biol 2007 17: 521–529. [PubMed: 17951048]
36. Mallevaey T, Clarke AJ, Scott-Browne JP, Young MH, Roisman LC, Pellicci DG, Patel O, Vivian JP, Matsuda JL, McCluskey J, Godfrey DI, Marrack P, Rossjohn J and Gapin L, A molecular basis for NKT cell recognition of CD1d-self-antigen. Immunity 2011 34: 315–326.
37. Wang J, Li Y, Kinjo Y, Mac TT, Gibson D, Painter GF, Kronenberg M and Zajonc DM, Lipid binding orientation within CD1d affects recognition of Borrelia burgorferi antigens by NKT cells. Proc Natl Acad Sci U S A 2010 107: 1535–1540. [PubMed: 20080535]
38. Hauser H, Short-chain phospholipids as detergents. Biochim Biophys Acta 2000 1508: 164–181.
39. Braun NA, Mendez-Fernandez YV, Covarrubias R, Porcelli SA, Savage PB, Yagita H, Van Kaer L and Major AS, Development of spontaneous anergy in invariant natural killer T cells in a mouse model of dyslipidemia. Arterioscler Thromb Vasc Biol 2010 30: 1758–1765. [PubMed: 20539017]
40. Parekh VV, Wilson MT, Olivares-Villagomez D, Singh AK, Wu L, Wang CR, Joyce S and Van Kaer L, Glycolipid antigen induces long-term natural killer T cell anergy in mice. J Clin Invest 2005 115: 2572–2583. [PubMed: 16138194]
41. Tahir SM, Cheng O, Shaulov A, Koezuka Y, Bubley GJ, Wilson SB, Balk SP and Exley MA, Loss of IFN-gamma production by invariant NK T cells in advanced cancer. J Immunol 2001 167: 4046–4050. [PubMed: 11564825]
42. Gately CM, Podbielska M, Counihan T, Hennessy M, Leahy T, Moran AP, Hogan EL and O'Keeffe J, Invariant Natural Killer T-cell anergy to endogenous myelin acetyl-glycolipids in multiple sclerosis. J Neuroimmunol 2013 259: 1–7.
43. Weismann D and Binder CJ, The innate immune response to products of phospholipid peroxidation. Biochim Biophys Acta 2012 1818: 2465–2475. [PubMed: 22305963]
44. Pereira CS, Sa-Miranda C, De Libero G, Mori L and Macedo MF, Globotriaosylceramide inhibits iNKT-cell activation in a CD1d-dependent manner. Eur J Immunol 2016 46: 147–153. [PubMed: 26426881]
45. Macedo MF, Quinta R, Pereira CS and Sa Miranda MC, Enzyme replacement therapy partially prevents invariant Natural Killer T cell deficiency in the Fabry disease mouse model. Mol Genet Metab 2012 106: 83–91. [PubMed: 22425450]
46. Ahaneku JE, Taylor GO, Olubuyide IO and Agbedana EO, Abnormal lipid and lipoprotein patterns in liver cirrhosis with and without hepatocellular carcinoma. J Pak Med Assoc 1992 42: 260–263. [PubMed: 1336073]
47. Kosicek M, Kirsch S, Bene R, Trkanjec Z, Titlic M, Bindila L, Peter-Katalinic J and Hecimovic S, Nano-HPLC-MS analysis of phospholipids in cerebrospinal fluid of Alzheimer's disease patients--a pilot study. Anal Bioanal Chem 2010 398: 2929–2937.

48. Mapstone M, Cheema AK, Fiandaca MS, Zhong X, Mhyre TR, Macarthur LH, Hall WJ, Fisher SG, Peterson DR, Haley JM, Nazar MD, Rich SA, Berlau DJ, Peltz CB, Tan MT, Kawas CH and Federoff HJ, Plasma phospholipids identify antecedent memory impairment in older adults. Nat Med 2014.

49. Kosinska MK, Liebisch G, Lochnit G, Wilhelm J, Klein H, Kaesser U, Lasczkowski G, Rickert M, Schmitz G and Steinmeyer J, A lipidomic study of phospholipid classes and species in human synovial fluid. Arthritis Rheum 2013 65: 2323–2333. [PubMed: 23784884]

50. Bandyopadhyay R and Basu MK, Involvement of PL-D in the alternate signal tranduction pathway of macrophages induced by an external stimulus. Mol Cell Biochem 2000 203: 127–133.

51. Bohdanowicz M, Schlam D, Hermansson M, Rizzuti D, Fairn GD, Ueyama T, Somerharju P, Du G and Grinstein S, Phosphatidic acid is required for the constitutive ruffling and macropinocytosis of phagocytes. Mol Biol Cell 2013 24: 1700–1712, S1701–1707. [PubMed: 23576545]

52. Mendiratta SK, Martin WD, Hong S, Boesteanu A, Joyce S and Van Kaer L, CD1d1 mutant mice are deficient in natural T cells that promptly produce IL-4. Immunity 1997 6: 469–477. [PubMed: 9133426]

53. Cui J, Shin T, Kawano T, Sato H, Kondo E, Toura I, Kaneko Y, Koseki H, Kanno M and Taniguchi M, Requirement for Valpha14 NKT cells in IL-12-mediated rejection of tumors. Science 1997 278: 1623–1626.

54. Aspeslagh S, Li Y, Yu ED, Pauwels N, Trappeniers M, Girardi E, Decruy T, Van Beneden K, Venken K, Drennan M, Leybaert L, Wang J, Franck RW, Van Calenbergh S, Zajonc DM and Elewaut D, Galactose-modified iNKT cell agonists stabilized by an induced fit of CD1d prevent tumour metastasis. EMBO J 2011.

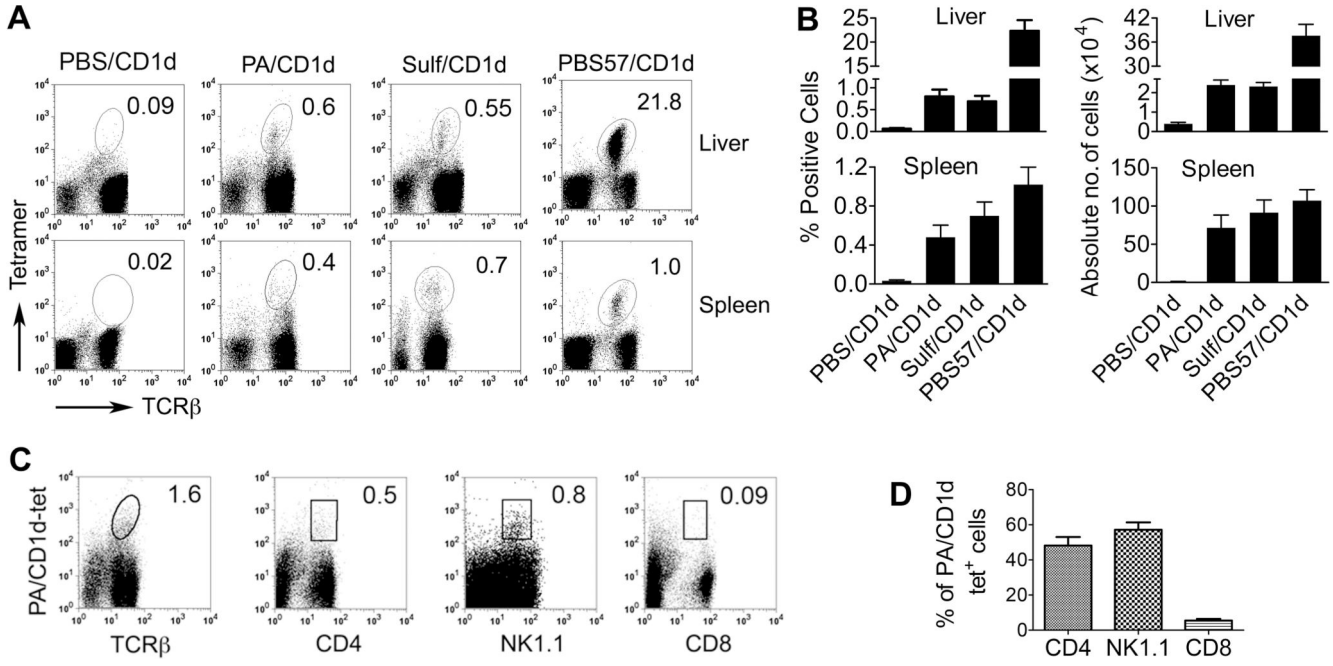

Figure 1. Detection of phospholipid-reactive T cells.

(**A**) Freshly isolated spleen and liver mononuclear cells from naïve B6 mice were stained with CD1d tetramers loaded with PBS (PBS/CD1d), a GPL Ag (phosphatidic acid [PA]), and glycosphingolipid Ag sulfatide (Sulf) and αGalCer (αGC)-analog PBS57. Stained cells were analyzed for iNKT cells (αGalCer-reactive T cells), dNKT (sulfatide-reactive T cells), and PLT (PA-reactive T cells) on gated live non-B lymphocytes. Numbers on plots indicate $TCR\beta^{+}tetramer^{+}$ cells as % of live lymphocytes. Dotplots shown are representative of more than five independent experiments, each using 2 to 4 mice. (**B**) Results are summarized as the mean ± SE % and absolute numbers of $tetramer^{+}$ cells (n = 5–8 mice, pooled from two separate experiments). (**C**) Liver MNCs from naïve B6 mice were stained with PA-loaded CD1d tetramer (PA/CD1d-tet) and Ab for the indicated markers, and analyzed for PLT cells. Numbers on plots indicate % positive of PA/CD1d-tet^{+} T cells. Results shown are representative of three independent experiments, each using 2 to 4 mice. (**D**) Percentages of PLT cells expressing various markers are expressed as the mean ± SE (n = 5 mice pooled from two experiments).

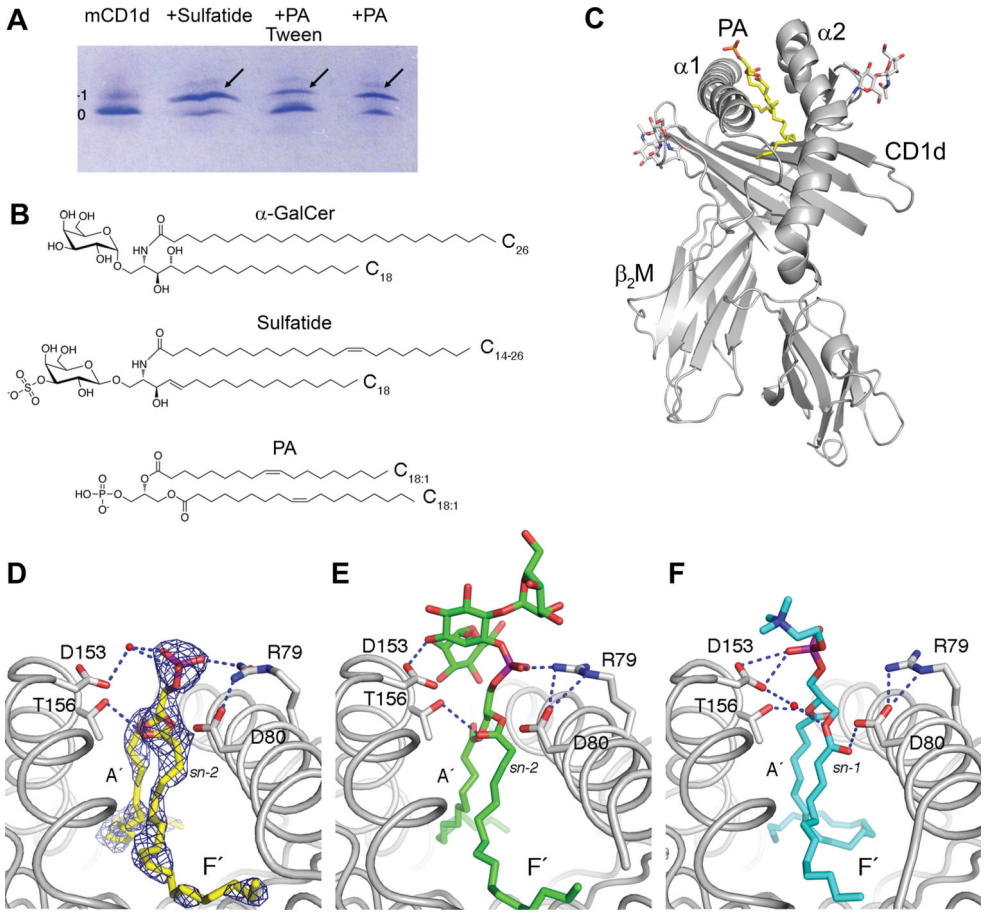

Figure 2. Binding and presentation of PA to mCD1d.

(**A**) Binding of synthetic dioleoyl-PA (PA) to mCD1d, as detected by native IEF gel electrophoresis. mCD1d (negative control) was incubated with sulfatide (positive control) or PA overnight at RT and successful lipid loading was visualized as a gel shift by native IEF. Notably, 0.05% Tween-20 in loading buffer reduces loading efficiency (+PA Tween). (**B**) Chemical structures of PA and the NKT cell ligands sulfatide and αGalCer (αGC). (**C**) Schematic representation of the mCD1d:PA complex showing PA bound between the α1 and α2 helix of CD1d, which non-covalently associates with β2-microglobulin. (**D**) Details of PA presentation by mCD1d. PA is oriented by H-bonds (blue dotted lines with distance of 3.5Å or less) by CD1d residues D153 (through water-mediated H bond), T156 and R79. Electron density for the ligand is depicted as blue mesh (2FoFc map contoured at 1 sigma). PA binds with *sn*-2 linked fatty acid in F' pocket, similar to the ligands phosphatidyl inositol dimannoside (PIM2) (**E**) and PC (**F**). The data are representative of two independent experiments.

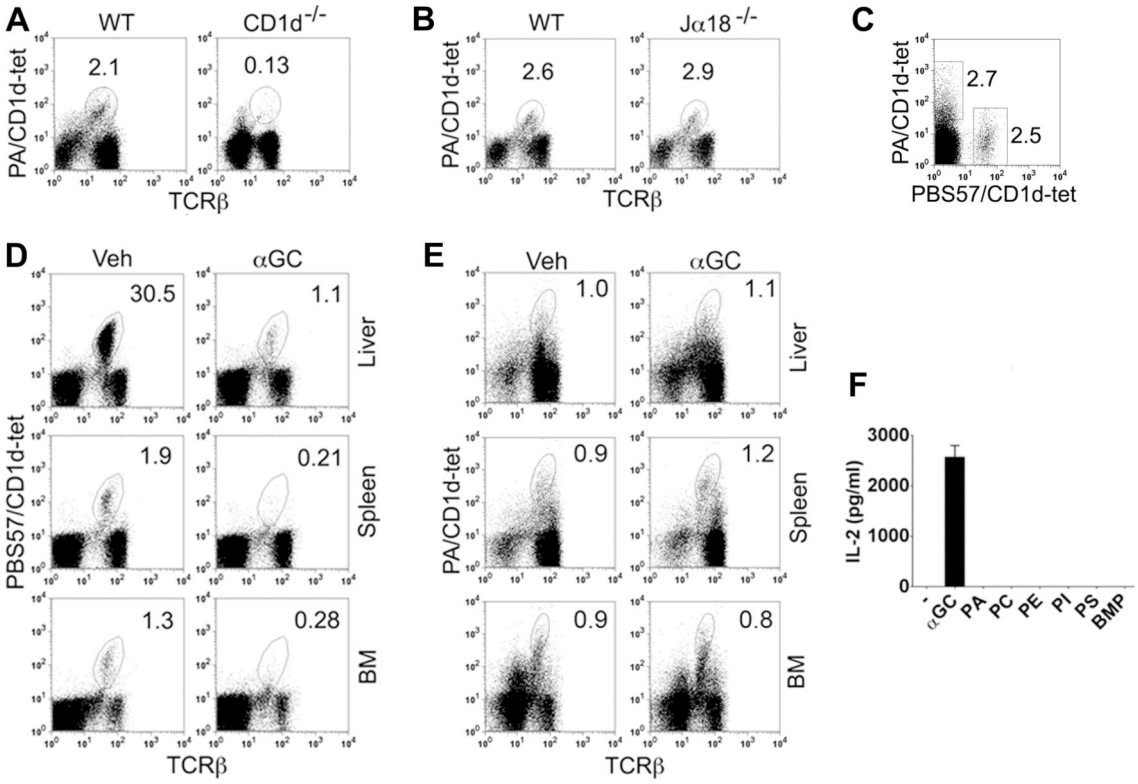

Figure 3. Characterization of phospholipid-reactive T cells.

(**A, B**) Spleen cells from B6 CD1d$^{-/-}$ and BALB/c Jα18$^{-/-}$ mice and their respective wild-type (WT) controls were analyzed for PLT cells. Numbers on plots indicate % TCRβ^{+}tetramer^{+} cells of live non-B lymphocytes. The data shown are representative of two (CD1d$^{-/-}$) and three (Jα18$^{-/-}$) independent experiments, each using 3 mice per group. (**C**) B6 spleen cells were stained with PE-labeled PA/CD1d and APC-labeled PBS57/CD1d tetramers, and analyzed for PLT and iNKT cells, respectively. Numbers on plots indicate % TCRβ^{+}tetramer^{+} cells of live TCRβ^{+} lymphocytes. Data shown are representative of four independent experiments, each using 2 to 3 mice per group. (**D, E**) B6 mice were injected with vehicle (*Veh*) or αGalCer (2 μg i.p.). Their liver, spleen and bone marrow (BM) were harvested 24 h later, and analyzed for iNKT (**D**) or PLT cells (**E**). Numbers on plots indicate % TCRβ^{+}tetramer^{+} cells of live non-B lymphocytes. The data shown are representative of three independent experiments, each using 2 to 3 mice per group. (**F**) PBS (–), αGalCer (10 ng/ml) or GPLs (20 μg/ml), including PA, PC, PE, PI, PS, and PG isomer BMP [bis(monoacylglycero)phosphate], were added to wells pre-coated with mCD1d, washed, and iNKT hybridoma cells added for 17 h. Supernatants were assayed for IL-2. The data shown are representative of three independent experiments.

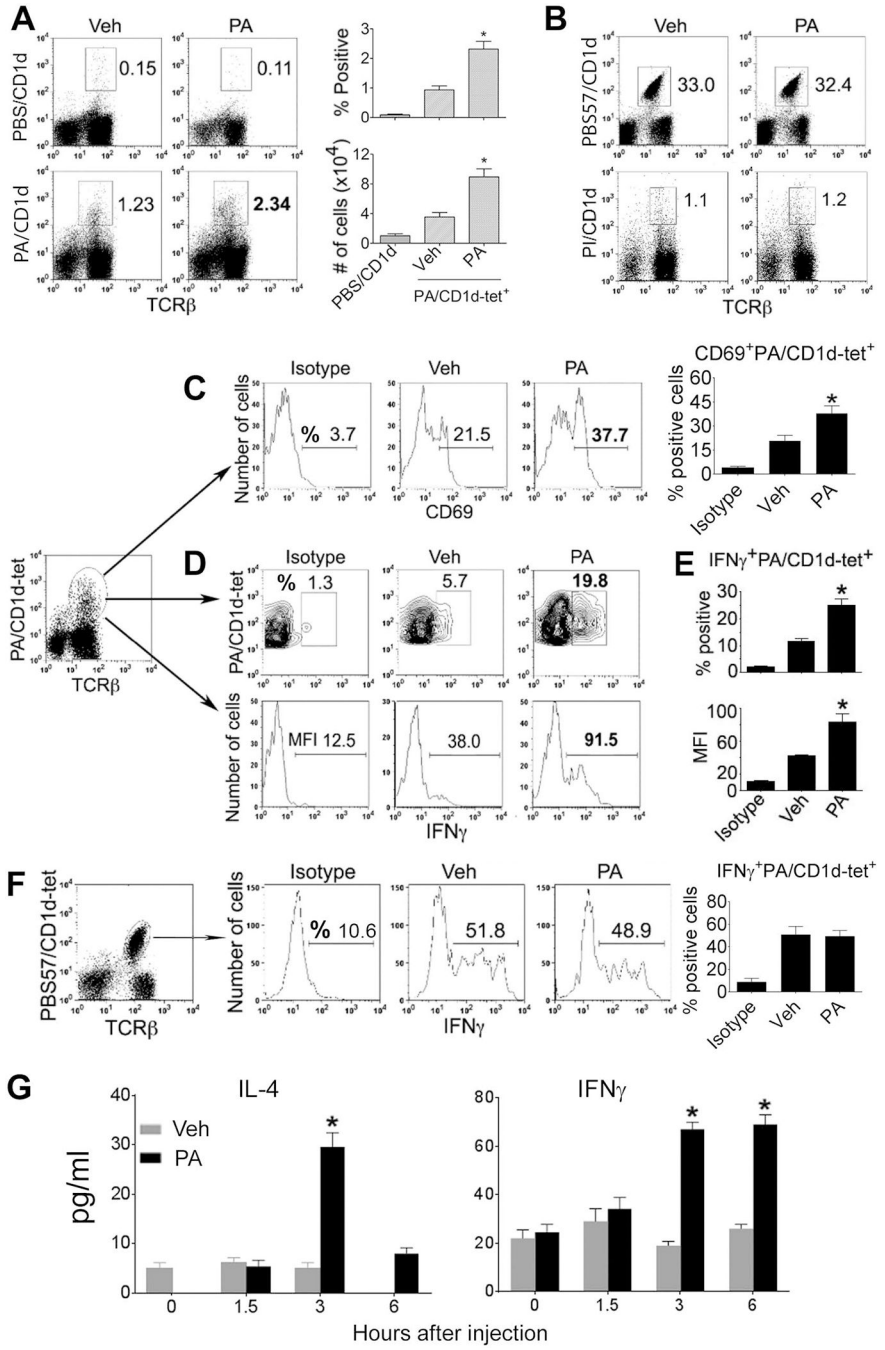

Figure 4. Effect of immunization with PA on PA-reactive T cells in vivo.

(**A**) B6 mice were injected with vehicle (*Veh*) or PA (20 μg i.p.), and liver was harvested 24 h later. Isolated liver MNCs were stained with CD1d tetramers loaded with PBS or PA. Numbers on plots indicate % TCRβ$^+$tetramer$^+$ cells of live non-B lymphocytes. Dotplots shown are representative of four independent experiments, each using 2 to 3 mice per group. Percent positive and absolute numbers of PA/CD1d-tet$^+$ cells from these animals are expressed as the mean ± SE in a bar diagram (*p <0.003; n = 9 mice/group, pooled from three experiments). (**B**) Liver MNCs from these animals were stained with CD1d tetramers

loaded with PBS57 and PI, and analyzed on live non-B lymphocyte gate. Numbers on plots indicate % TCRβ$^+$tetramer$^+$ cells of live non-B lymphocytes. Data shown are representative of three experiments. (**C**) PA/CD1d-tet$^+$ T cells from these animals were analyzed for CD69 expression (*p <0.0001; n = 9 mice/group; mean ± SE). (**D**-**F**) Liver MNCs isolated 24 h after a PA or vehicle injection were cultured for 5–6 h with 500 ng/ml ionomycin and 10 ng/ml PMA in presence of Golgi-plug (1 μl/ml), and cells analyzed for intracellular cytokines. Results of IFNγ production on gated TCRβ$^+$ PA/CD1d-tet$^+$ cells (**D, E**) or gated iNKT cells (**F**) are shown. Numbers on histograms represent % positive cells or MFI, as indicated. Data in (**E**) are presented as the mean ± SE % positive and MFI of IFNγ on gated PA/CD1d-tet$^+$ cells (*p <0.002; n = 6 mice/group, pooled from three experiments). Data shown are representative of three independent experiments. (**G**) B6 mice were injected with vehicle (*Veh*) or PA (20 μg i.p.), and bled at the indicated timepoints. Their serum samples assayed by ELISA for cytokines (*p <0.001; n = 6–8 mice/timepoint, pooled from three separate experiments; mean ± SE).

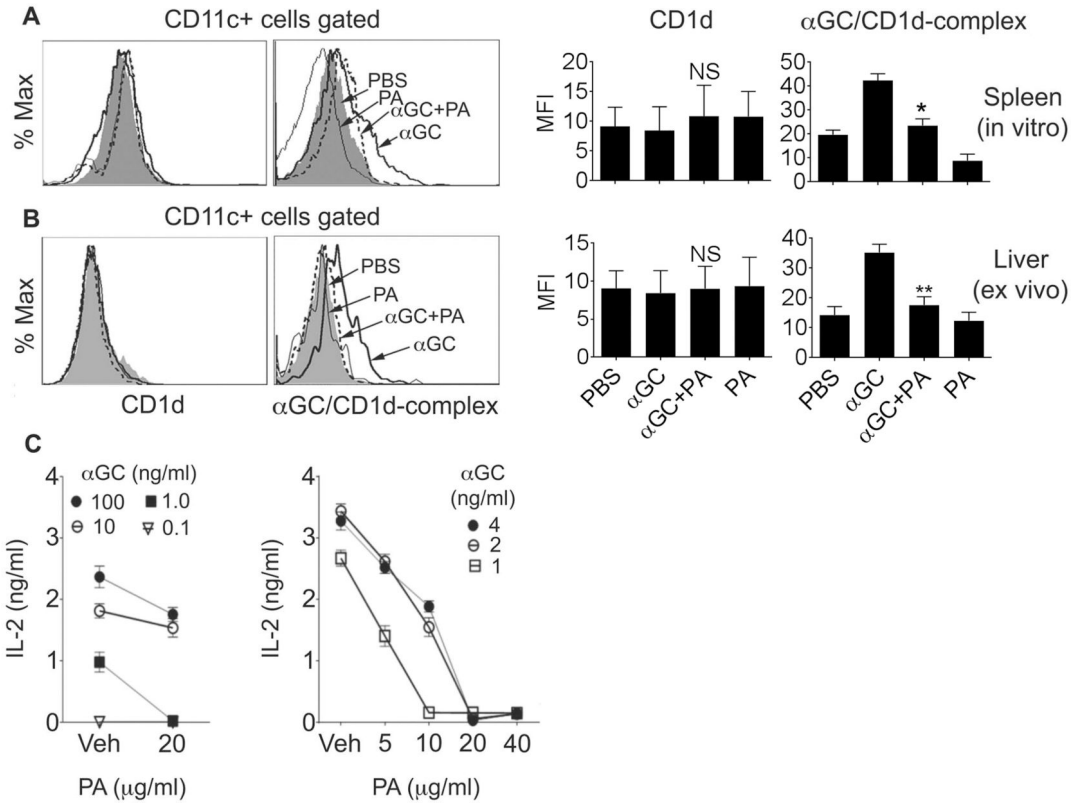

Figure 5. PA competes with αGalCer for loading onto CD1d and presentation.

(**A**) Spleen cells were incubated with PBS (filled histogram), PA (20 μg/ml, gray line), αGalCer (αGC) (100 ng/ml, thick line) or PA + αGalCer (dashed line) for 20h. Cells were then stained with anti-CD1d or anti-CD1d:αGalCer complex (clone 363) and anti-CD11c Ab. Surface expression of CD1d and CD1d:αGalCer complexes on DCs ($CD11c^+$) is shown in left and right panels, respectively. The data shown are representative of three independent experiments, each using cells from one animal. Combined data with statistics are shown in the bar diagrams (*$p < 0.001$; $n = 3$). (**B**) B6 mice were injected with PBS (filled histogram), PA alone (gray line), αGalCer alone (thick line), or PA + αGalCer (dashed line). Animals were euthanized at 24h, and isolated liver leukocytes stained with Ab against CD1d or CD1d:αGalCer complex and CD11c. Stained cells were analyzed for surface expression of CD1d (left panels) or CD1d:αGalCer complexes (right panels) on DCs. Note the reduced expression of CD1d:αGalCer complexes on DCs in animals injected with PA + αGalCer as compared to animals injected with αGalCer alone. The data are representative of two independent experiments, each using three mice per group. Combined data with statistics are shown in the bar diagrams (**$p<0.01$; $n = 3$). (**C**) Plates were coated with soluble mCD1d and washed after 18 h. αGalCer at different concentrations was then added to these plates, followed immediately by addition of vehicle (*Veh*) or PA at concentrations indicated on figure panels. Plates were washed after 4 h, and iNKT hybridoma cells added. Supernatants collected after 17 h were tested for IL-2. Results are expressed as the mean ± SD of the mean triplicate values of IL-2. Similar results were obtained in another set of experiments using PA and αGalCer concentrations used in both panels.

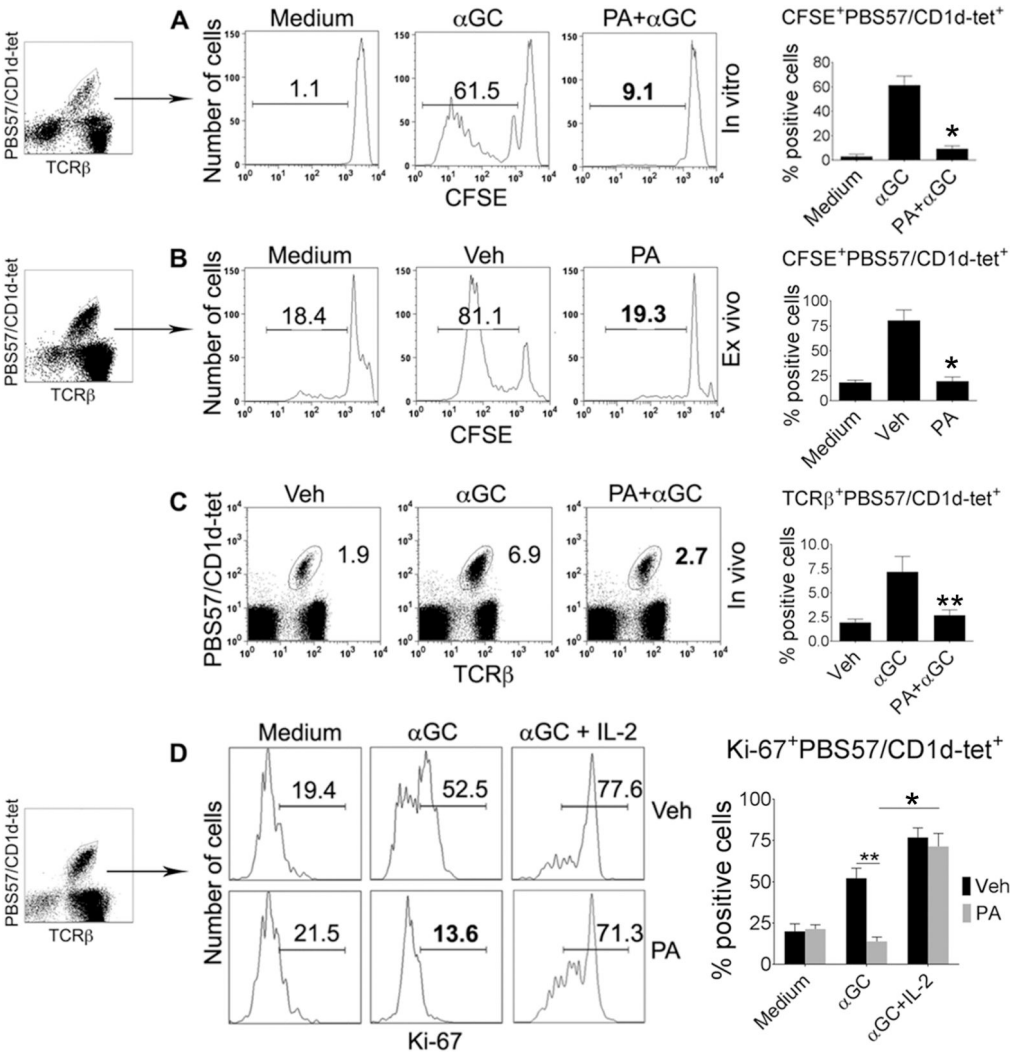

Figure 6. Effect of PA on iNKT cell proliferation.

(**A**) Spleen cells from B6 mice were labeled with CFSE, and cultured with medium alone, αGalCer (αGC), or PA+αGalCer for 4 d at 37°C. iNKT cell proliferation was assessed by CSFE dilution in PBS57/CD1d-tet^{+} TCRβ^{+} live B220^{-} lymphocytes. Numbers on plots indicate % positive cells. The data are representative of five independent experiments, each using spleen cells from one animal. (**B**) B6 mice were injected with PA or vehicle (*Veh*), and spleen harvested after 24 h. Spleen cells were labeled with CFSE, cultured with αGalCer for 4 d, and CFSE dilution analyzed on iNKT cells. The data are representative of five independent experiments, each using 3 mice per group. (**C**) B6 mice were injected with vehicle, αGalCer, or PA+αGalCer. Spleen cells isolated from these animals were analyzed for PBS57/CD1d-tet^{+} TCRβ^{+} cells on gated live B220^{-} lymphocytes. The data shown are representative of three independent experiments, each using 3 to 4 mice per group. (**D**) B6 mice were injected with PA or vehicle, and spleen harvested 12h later. Spleen cells were cultured with medium alone, αGalCer or αGalCer+IL-2 for 4 d, and Ki-67 analyzed on iNKT cells. The data are representative of three independent experiments, each using 3 mice

per group. Combined data with statistics are shown in the bar diagrams (*p <0.001, **p<0.01; n = 3–5).

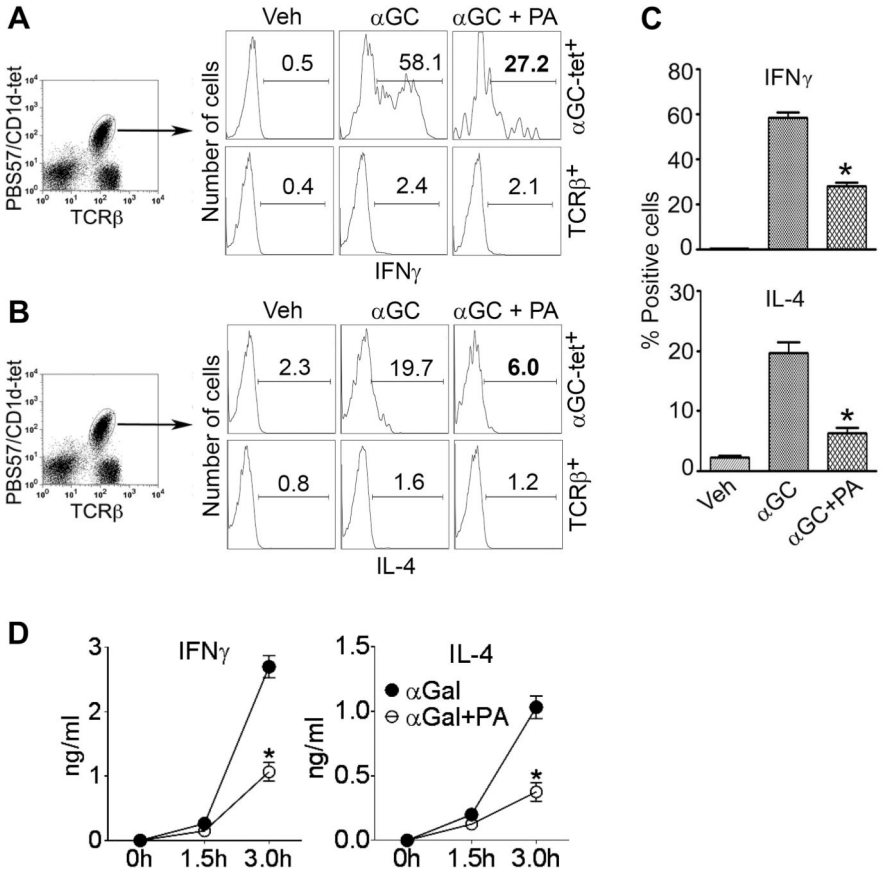

Figure 7. Effect of PA on cytokine production by iNKT cells.

B6 mice were injected with PA (20 μg i.p.) + αGalCer (2–4 μg i.p.) or αGalCer (αGC) alone, and animals were euthanized 3 h later. Liver MNCs were isolated and analyzed for intracellular cytokines. Representative histograms show IFNγ$^+$ (**A**) and IL-4$^+$ (**B**) cells on gated iNKT cells (PBS57/CD1d tetramer$^+$ TCRβ$^+$; upper panels) or conventional T cells (tetramer$^-$TCRβ$^+$; lower panels) from one of three independent experiments, each using 2 mice per group. Results are summarized in panel (**C**) (*p <0.004; n = 6 mice/group, pooled from three experiments; mean ± SE). (**D**) B6 mice were injected with αGalCer or αGalCer +PA, and animals bled at the indicated time points. Serum samples were assayed for cytokines by ELISA (*p =0.003; n = 6 mice/group, pooled from two separate experiments; mean ± SE).